



ISSN: 0067-2904

Influence of Acid Activation of a Mixture of Illite, Kaolinite, and Chlorite Clays on the Adsorption of Methyl Violet 6B Dye

Saba Adil Saed , Dunya Edan AL-Mammar

Department of Chemistry, College of Science, University of Baghdad, Baghdad, Iraq

Abstract

The influence of acid activation of a mixture of illite, kaolinite, and chlorite clays collected from the area of Zorbatiya (east of Iraq) on the adsorption of methyl violet 6B (MV6B) as a cationic dye was studied. The activation was carried out by using 0.25M HCl and 0.25M H₂SO₄. Raw and acid-activated clays were analyzed by atomic force microscopy (AFM), scanning electron microscopy (SEM), and X-ray diffraction (XRD).

Batch adsorption method was used to study the adsorption of MV6B onto the raw and acid activated clays. The impacts of different factors on the adsorption process were studied, such as clay weight, agitation time, starting MV6B concentration, temperature, ionic strength, and solution pH. The adsorption process was described by using Langmuir, Freundlich, Temkin, and Dubinin- Radushkevich isotherm models. Thermodynamic parameters like ΔH°_a , ΔS°_a , and ΔG°_a were estimated based on Van't Hoff equation.

Keywords: Adsorption MV6B dye, raw clay, acid activated clays.

تأثير التنشيط بالحامض لمزيج من أطيان أليليت والكاوليت والكلوريت على إمتزاز صبغة المثيل البنفسجي (6ب)

صبا عادل سعيد, دنيا عيدان المعمار

قسم الكيمياء, كلية العلوم, جامعة بغداد, بغداد, العراق

الخلاصة

تمت دراسة تأثير التنشيط بالحامض لمزيج من أطيان أليليت والكاوليت والكلوريت من منطقة زرباطية (شرق العراق) على إمتزاز صبغة المثيل البنفسجية 6ب كصبغة كاتيونية. تم التنشيط باستخدام (0,25) مولاري حامض الهيدروكلوريك و(0,25) مولاري حامض الكبريتيك. تم تحليل الاطيان الخام والمنشط بالحامض باستخدام مجهر القوة الذرية (AFM) ومجهر المسح الالكتروني (SEM) وحيود الاشعة السينية (XRD).

أُستخدمت طريقة الوجبة للامتزاز لدراسة امتزاز صبغة المثل البنفسجي 6ب على سطح الطين الخام والطين المنشط بالحامض. ثم دراسة تأثير مختلف العوامل على عملية الامتزاز مثل: وزن الطين، زمن الرج، التركيز الابتدائي لصبغة المثيل البنفسجي 6ب، درجة الحرارة، القوة الايونية ودرجة حامضية المحلول. جرى وصف عملية الامتزاز باستخدام نماذج متساوي درجة حرارة الامتزاز لنكامير، فرنشلز، وتمكن، ودوبن رادش كفيج. الدوال الترموديناميكية مثل ΔH°_a , ΔS°_a , ΔG°_a تم تقديرها بالاستناد الى معادلة فانث هوف.

1- Introduction

Dyes are organic colored substances used for coloring wool, textiles, paper, fibers, and leather [1]. Most of these dyes were designed to be resistant to the different environmental conditions, such as microbial attack and the effects of pH and light [2]. Also, small amounts of these substances in water were reported to cause dermatitis, allergy, mutations, and skin irritation for humans [3]. Therefore, the removal of these compounds from waste-effluents becomes a major issue. There are various chemical and physical processes which are available for the treatment of wastewater, including flocculation, ion-exchange precipitation, ozonation, and irradiation [4]. Among these different processes, adsorption should be one of the most effective techniques for the removal of color pollutants due to the cheapness, convenient operating conditions, and simple design [5]. There is a wide range of adsorbent materials employed for conditioning water, such as agricultural wastes [6], activated carbon, clay [7], and fly ash [8]. Using clays over commercially appropriate adsorbents have been well known, because they are abundant, non-toxic, and cost effective materials. Bentonite [9] reported that montmorillonite, semectite, Kiolinite, and illite [10] were used for the deportation of toxic metals and dyes. The clays are often modified by a thermal [11] or chemical treatment [12] to enhance their adsorptive characteristic. The aim of this study is to investigate the influence of acid-activation with HCl and H₂SO₄ on the adsorption behaviors of a mixture of illite, kaolinite, and chlorite clays sampled from the region of Zorbatiya (east of Iraq).

2-Materials and Methods

2-1- Materials

Methyl violet 6B (MV6B), a cationic dye with the chemical formula C₂₃H₂₆N₃Cl and molar mass of 379.94 g/mole, was provided from BDH. The molecular structure of the dye is illustrated in Figure-1. This dye is widely used in textile, paints, and printing industries owing to its distinctive dark violet color [13].

Stock solution of 1000 mg/L was prepared by dissolving 1g of MV6B in 1L distilled water. This solution used for the preparation of the working solutions by dilution until obtaining the desired concentration.

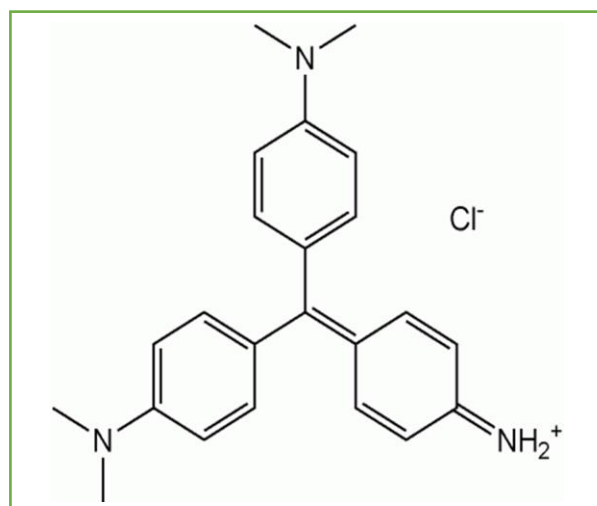


Figure 1- Chemical formula of methyl violet 6B dye

The raw clay used in the study was collected from Zorbatiya area (east of Iraq). The clay has the following composition: SiO₂ 19.6%, Al₂O₃ 3.8%, Fe₂O₃ 4.5%, C_aO 15.2%, MgO 3.4%, K₂O 1.3%, Na₂O 12.8%, TiO₂ 0.6%, P₂O₅ 0.1%, SiO₃ 1.2%, Cl 14.8%, M_nO 0.38% and L.O.I. 19.6%. The mineral analysis of this clay showed that it is a mixture of illite, kaolinite, and chlorite [14]. Acidification of the clays was performed by using 37% hydrochloric acid and 98% sulfuric acid supplied by Fluka.

2-2-Methods

30 g of the raw clay was mixed with 100 ml distilled water, followed by shaking for one hour at room temperature, and filtration by using Buckner funnel. The mixture was oven dried at 120°C for 7 hours, then allowed to cool and kept in a dry place. The obtained clay was labeled as RC.

2-2-1- Activation with HCl and H₂SO₄

To prepare acid-activated clay with HCl, a weight of 20 g of the raw clay was mixed with 67 ml 0.25 M HCl by using a thermostated shaker (Gallenkamp, England) for 2 hours. The resulting clay was filtered by using a Buckner funnel and the residue slurry was washed with distilled water until it became neutral. The prepared sample was dried at 120 °C for 2 hours and the activated clay was calcinated in muffle furnace (BS32C, Korea) at 750°C for 4 hours. The obtained clay was labeled as ACH.

The acid-activated clay with H₂SO₄ was prepared by mixing 20g of raw clay with 200 ml 0.25 M H₂SO₄ in a shaking water bath for 6 hours at 70°C. Then, the sample was allowed to stand for fourteen hours in solution. Finally, the precipitate was filtered and washed for many times with distilled water till reaching a natural pH. The sample was dried at 120°C for 2 hours, then calcinated at 750°C for 4 hours. The obtained clay was marked as ACS.

2-3-Batch adsorption studies

Batch experiments were carried out to study the adsorption of MV6B on RC and both acid-activated clays of ACH and ACS. A known quantity of the clay was added to 20 ml dye solution in 100 ml Erlenmeyer flask. The mixture was agitated by using a shaker with water bath (JTYS-1000, China) at pre- determined speed, time, and temperature. Centrifugation with 1000 rpm was used for 5 min to separate the supernatant. The residual MV6B dye concentration was determined by UV-Vis – Spectrophotometer (Shimadzu UV 1800, Japan) at $\lambda_{max} = 583$ nm.

The removal percentage R% and the amount of the MV6B dye adsorbed Q_e were calculated by using equations:

$$R\% = 100 \left[\frac{C_s - C_e}{C_s} \right] \quad \text{----- (1)}$$

$$Q_e = \frac{V}{M} [C_s - C_e] \quad \text{----- (2)}$$

where Q_e (mg/gm) is the amount of MV6B dye adsorbed on the clays at equilibrium, C_s, C_e are the starting concentration and the concentration at equilibrium (mg/L), respectively, V is the volume of the working solution (L), and M is the mass of the clay (g).

Results and discussion

3- Characterization

3-1- Morphology

3-1-1- Atomic force microscopy

The measurements of the average grain size were performed by AFM examination. Figures- 2, 3, and 4 display a typical surface from AFM images (in three dimensions), and the granularity cumulating distribution for three types of clays. The average diameter values for RC, ACH, and ACS were 160.52nm, 106.81nm, and 92.75nm), respectively. This indicates that the particle size of the acid-activated clays is smaller than that of the raw clay, which leads to increase the specific surface area for both ACH and ACS clays.

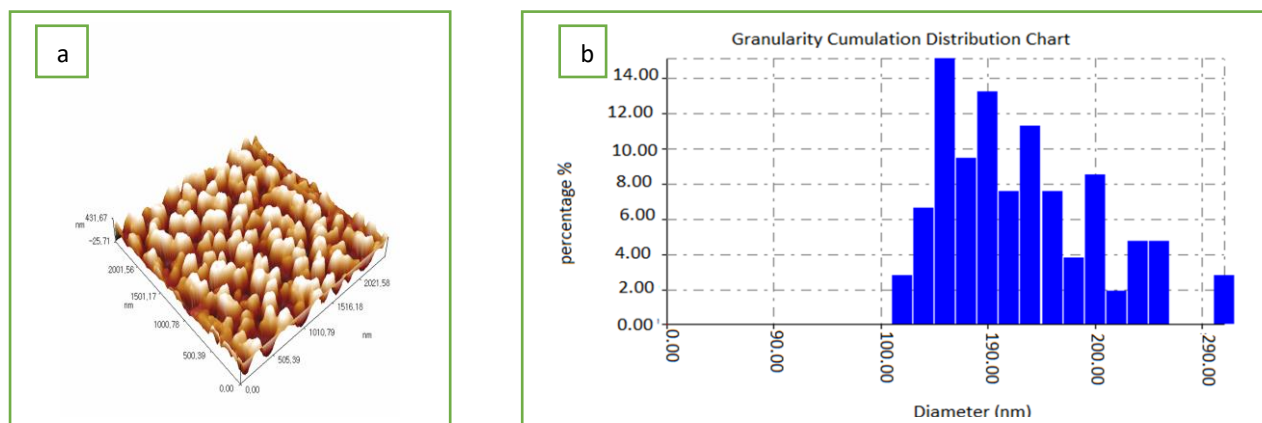


Figure 2 a- View of AFM image of RC; b: Granularity cumulating distribution chart of RC.

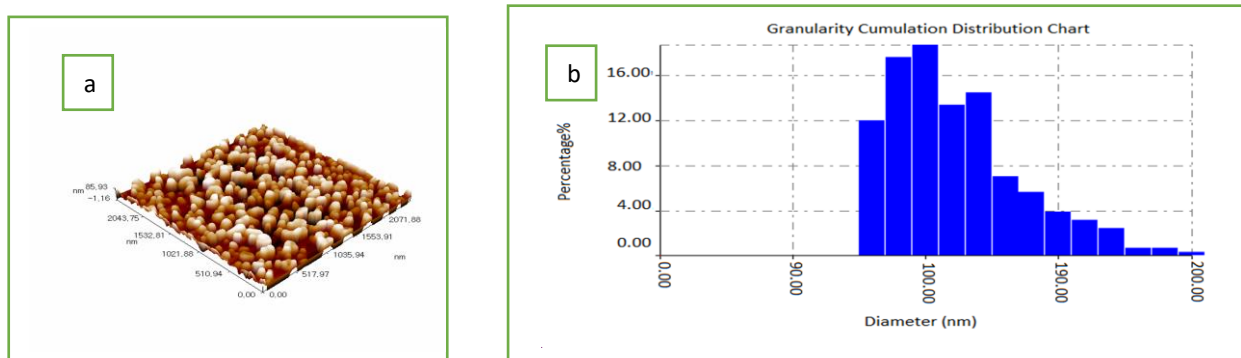


Figure 3- a View of AFM image of ACH; b: Granularity cumulating distribution chart of ACH.

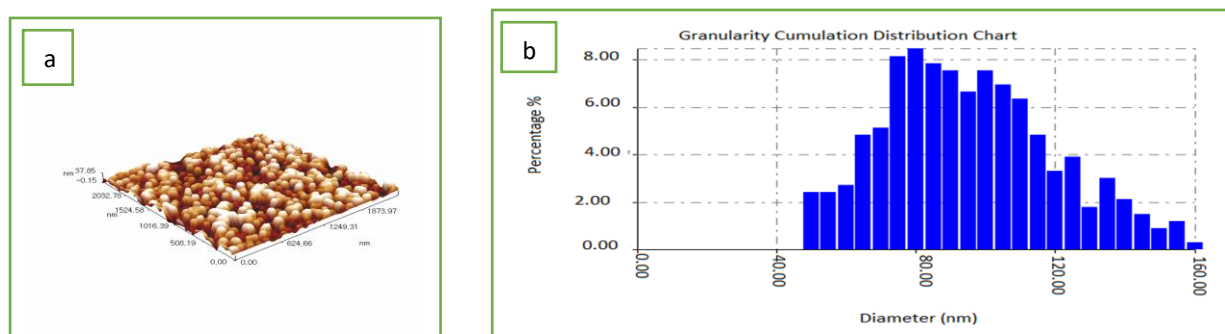


Figure 4 a- View of AFM image of ACS; b: Granularity cumulating distribution chart of ACS.

3-1-2- Scanning electron microscopy

The RC and acidactivated clay samples were tested under scanning electron microscopy (ZEISS Gemini-Germany) to explore the morphology, surface features, crystalline structure, and porosity. As shown in Figure -5 (a, b and c), the acid-activated clays with both HCl and H₂SO₄ are more porous than the raw clay. This may be attributed to the cation leaching from the clay surface in the course of its activation with acids, which creates voids on the clay, hence the clay surface becomes highly porous [15]. Also, this figure shows flake clustered particles with a smooth irregular surface [10].

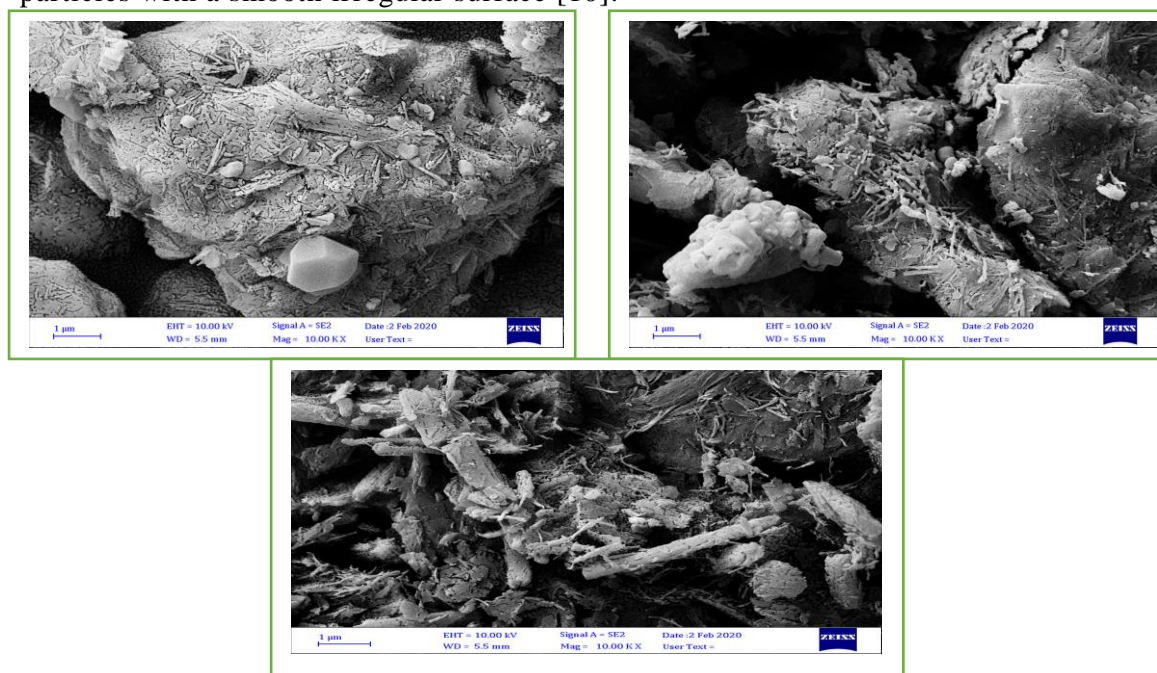


Figure 5- SEM images of clays surfaces for (a) RC, (b) ACH, and (c) ACS.

3-2- X-Ray diffraction

The XRD analysis was carried out by using x-ray diffraction detector(PNA analysis, XRD-UK). Figure- 6 (a, b and c) shows the XRD shapes for clay samples. It is obvious from Figure- 6(a) that the diffraction shape displays the existence of peaks related to quartz ($2\theta=26.637, 50.100$ degrees), calcite ($2\theta=29.412, 39.400, 47.540$ degrees), kaolinite ($2\theta=12.487, 24.321$ degrees), and illite ($2\theta=35.990$ degree). While for the acid-activated clay shown in Figure- 6(b, c), the peaks of kaolinite and illite become unimportant and the peaks of quartz and calcite become more concentrated [16].

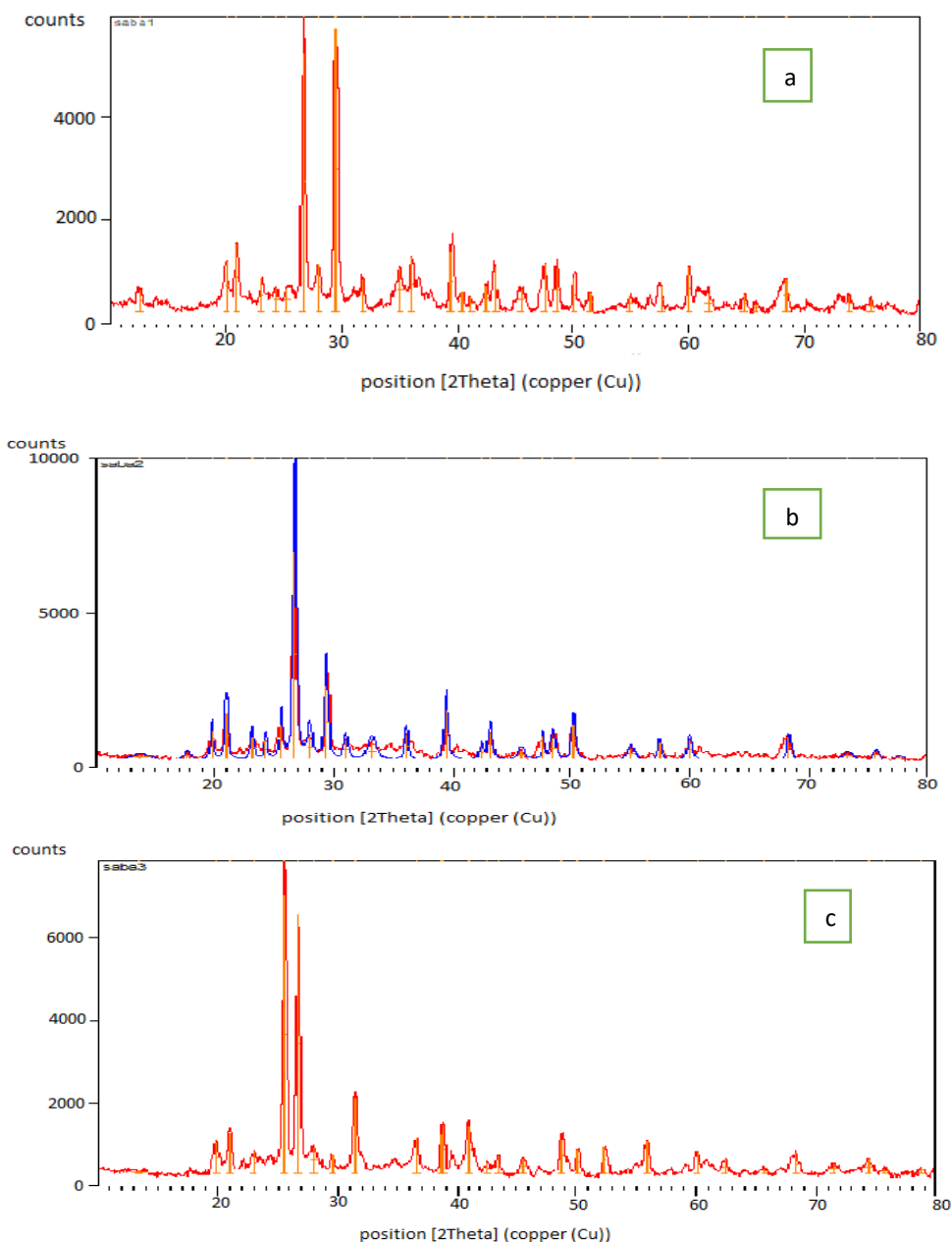


Figure 6-X- ray diffraction investigations of (a) RC, (b) ACH, and (c) ACS.

4- Influence of various parameters on MV6B adsorption

4-1- Influence of clay dosage

The influence of clay dosage on the removal of MV6B dye from RC, ACH, and ACS clays was tested by using various amounts of clay (in the range of 0.025-0.5 g) and 20 ml of 10 mg/L MV6B dye at 293 K, pH 7, and shaking speed of 150 rpm. As shown in Figure-7, the removal percentage for the three types of clay increased from 6.35 to 96.62% for RC and from 7.7 and 8.7% to 99.1 and 99.72% for ACH and ACS, respectively, with the increase in clay dosage. Thus, in the higher dosage, the clay provides more active surface sites [19]. However, further increasing the clay weight did not show any

increase in the removal percentage . This is due to the overlapping between the active sites at high amounts of adsorbent. Similar results were reported by Zhang *et al.* [20]. Therefore, 0.1 g of clay was selected as an optimum dosage.

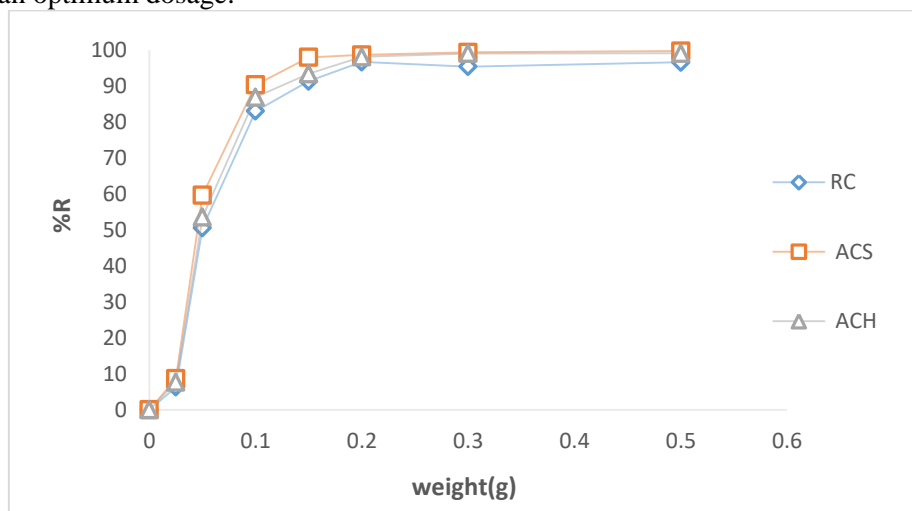


Figure 7- Influence of clay dosage on the removal percentage (R%) of MV6B dye.

4-2- Influence of agitation time

The influence of agitation time on the removal percentage of 10 mg/L MV6B dye by using raw and acid activated clays was tested at pH 7, range of time of 5-60 min, temperature of 293K, clay dosage of 0.1g, and agitation speed of 150 rpm. It is clear from Figure-8 that the removal percentage suddenly increases at 5 min and then onwards a steady state is reached. This may be attributed to the obtainability of empty adsorption sites on the surface of the clay, which is slowly increased until reaching equilibrium [13]. Thus, the optimum time chosen was 45 min.

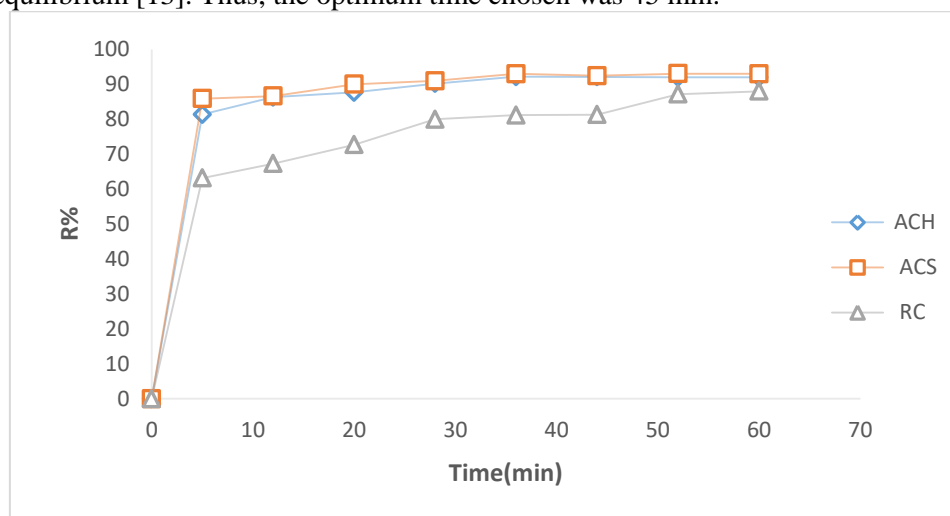


Figure 8- Influence of agitation time on the adsorption of MV6B dye onto raw and acid activated clays.

4-3- Influence of starting dye concentration

The influence of starting MV6B concentration was tested at the following conditions: dye concentration ranging 10, 20, 30, 35, and 40 mg/L, clay dosage of 0.1 g, pH 7, temperature of 293K, agitation time of 45 min, and shaking speed of 150 rpm. It is obvious from Figure-9 that as MV6B concentration starts to change from 10 to 40 mg/L, R% values change from 80.24 to 65.38 for raw clay and from 82.1 and 85.01 to 66.23 and 66.73 for the acid activated clays of ACH and ACS. These results may be accounted to that, at low MV6B dye concentration, sufficiently available active sites are present on the clay surfaces, while upon increasing dye concentration, the demand for active sites is higher, but the available ones are limited [21].

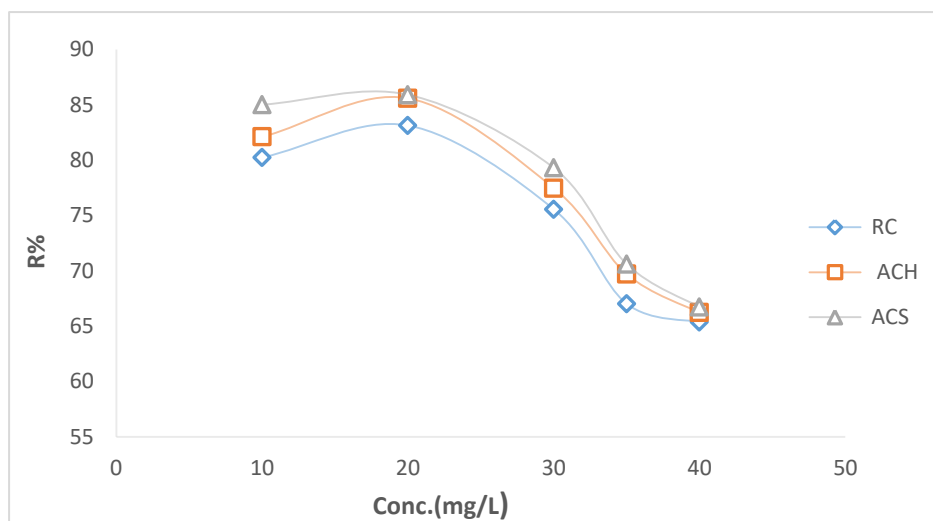


Figure 9- Influence of starting MV6B concentration on the adsorption of MV6B dye onto RC and acid activated clays.

4-4- Temperature influence

The temperature influence on the percentage removal of MV6B was examined by changing the temperature from 288K to 328K at the following optimum conditions: starting concentration of MV6B 10 mg/L, pH 7, clay dosage of 0.1 g, time for equilibrium of 45 min, and shaking speed of 150 rpm. The results are depicted in Figure-10. It can be reported that the R% increased with rising temperature, which reflects the endothermic nature for the adsorption process.

The noted influence refers to an increase in the mobility of the MV6B dye that leads to an increase in the number of active adsorption sites with rising temperature. This may causes an increase in the number of molecules that have sufficient energy for the interaction with the active surface sites. Additionally, when temperature increases, it causes swelling in the internal structure of clay, which allows for a large dye molecules to penetrate the surface of clay [21].

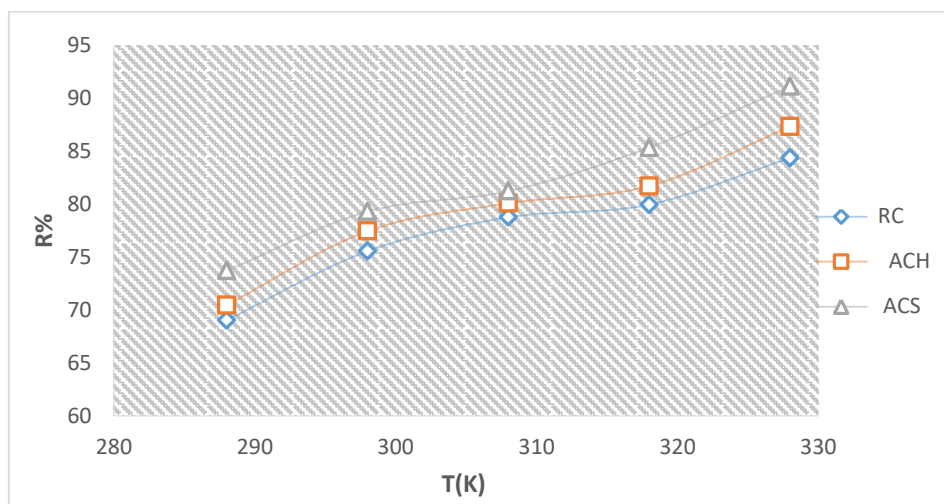


Figure 10- Temperature influence on the adsorption of MV6B onto different adsorbents.

4-5- Influence of solution ionic strength

The impact of ionic strength on the MV6B adsorption was studied by adding sodium chloride salt within the range of 0.2-1.0 mg/L, with a starting MV6B concentration of 10mg/L, clay dosage of 0.1 g, pH 7, shaking time of 45 min, temperature of 293K and shaking speed of 150 rpm. Figure- 11(a) indicates that the R% of MV6B dye onto raw clay is decreased when the concentration of NaCl is increased. This phenomenon can be ascribed for two factors; first, the cation of Na^+ contest with the cations of the dye on the negatively charged sites in the adsorbent surface; second, the Cl^- ions

counterbalance the cationic charge of the dye molecules and shield the electrostatic attraction between them and the anionic clay surfaces. As a result, the adsorption of cationic dyes onto the negatively charged sites of clay surfaces is inhibited by high concentrations of NaCl [13]. Figure 11(b) shows that the R% of the absorption of MV6B dye onto acid activated clays is increased with the increase in the concentration of NaCl. This may be related to the accumulation of cations of MV6B dye persuaded by the action of salt ions. Several types of intermolecular forces were proposed to affect this aggregation, including van der Waals, ion dipole, and dipole-dipole forces. These forces occur between dye molecules in the solution and they are increased when NaCl salt is added to the MV6B solution [22].

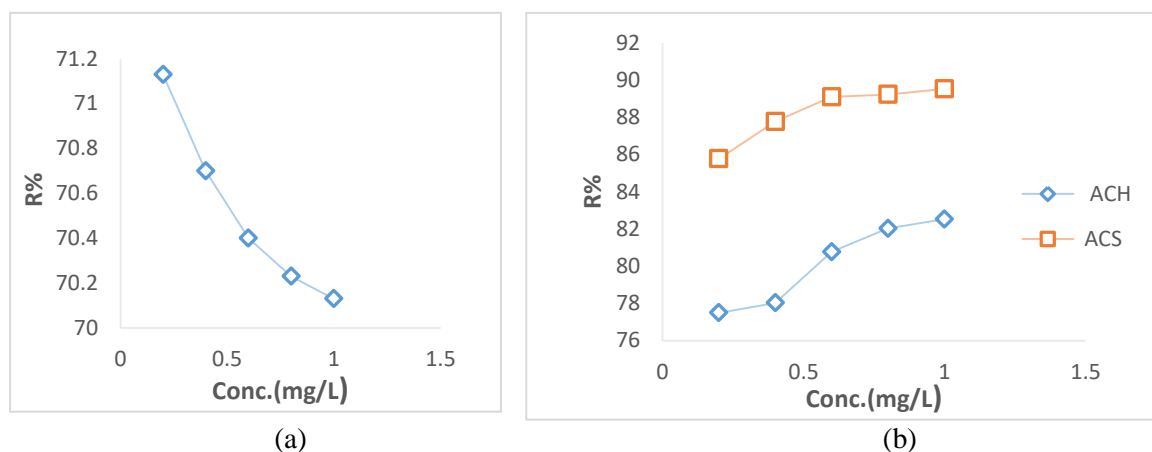


Figure 11- Influence of ionic strength on the adsorption MV6B onto (a) RC; (b) ACH and ACS.

4-6- Influence of initial pH

The impact of pH was investigated in the course of its variation between 1.67 and 11 at 293K, starting concentration of 10 mg/L, 0.1 g clay dosage, agitation time equal to 45 min, and shaking speed equal to 150 rpm. The pH of the solution was adjusted by using 1M HCl and 1M NaOH, was and the results are illustrated in Figure-12. It is evident that the percentage of the adsorption of MV6B dye onto RC, ACH, and ACS increases with increasing the pH of the solution. The low value of R% for these clays at low pH is related to the competition between the MV6B ions and hydrogen ions for the acid. If the pH values exceed 7, the R% is growing rapidly till it reaches 70.69 for RC and 73.26 and 79.49 for ACH and ACS, respectively. Hence, it is clear that the MV6B produces cations in the aqueous medium. Thus, the adsorption of the cationic dye on the clays surfaces is primarily affected by the charge of the clay surface. At lower pH, there is an electrostatic repulsion between the MV6B ions and the positive charge groups on the clay surfaces, while at a higher pH, the clay surface becomes negative that leads to decrease the electrostatic repulsion and, hence, the dye cations in solution can be attracted to the surface [17].

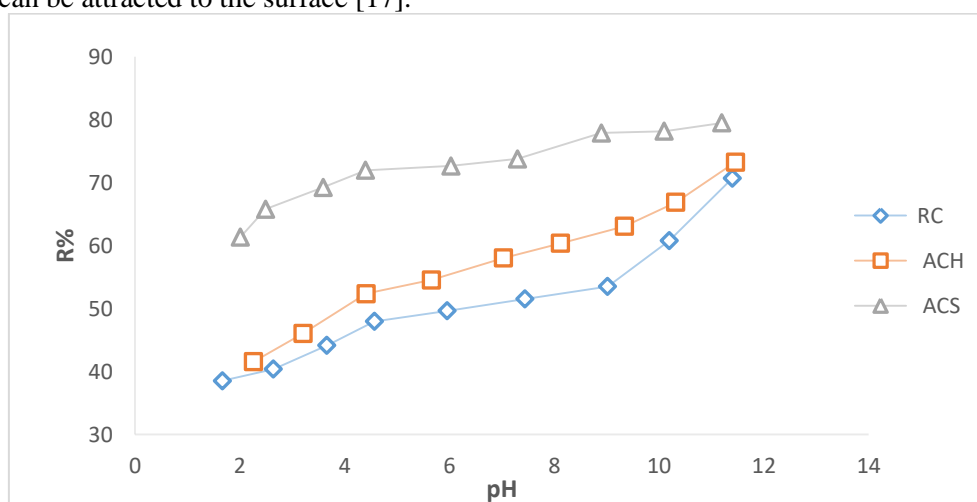


Figure 12- Influence of pH on the adsorption of MV6B dye onto raw clay and acid activated clays.

5- Isotherm modeling

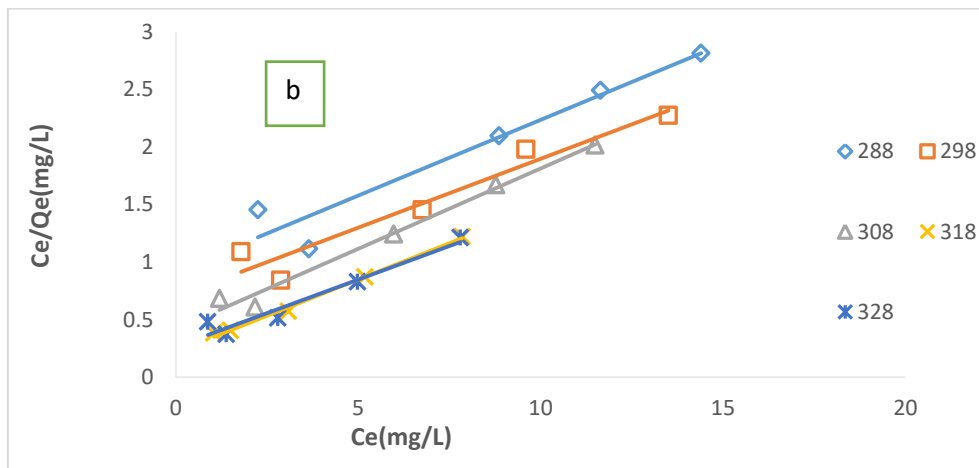
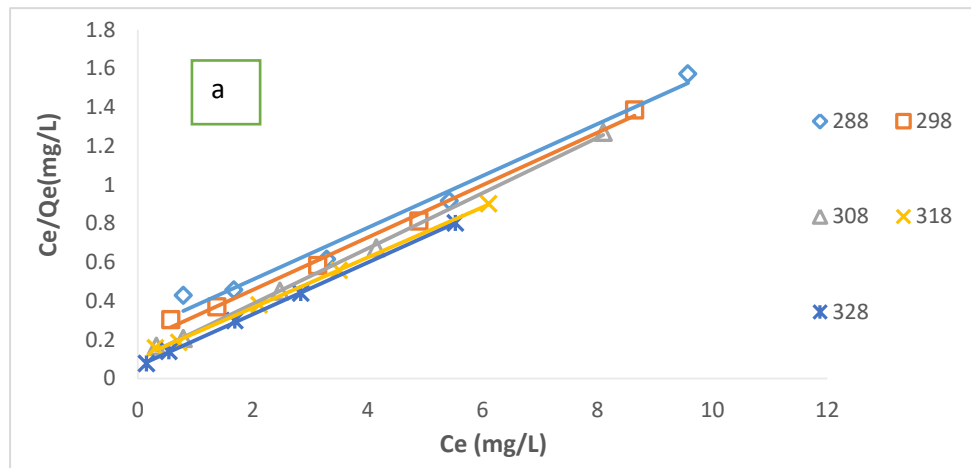
The adsorption was analyzed by using Langmuir, Freundlich, Temkin and Dubinin-Radushkevich models.

5-1- Langmuir isotherm

The Langmuir isotherm model postulates the maximum adsorption of a saturated monolayer of solute molecules on the adsorbent surface. The linear form of Langmuir model is [23]:

$$\frac{C_e}{Q_e} = \frac{1}{Q_m \cdot k_L} + \frac{1}{Q_m} \cdot C_e \tag{3}$$

Q_m (mg/g) and k_L (L/mg) are the Langmuir constants associated to adsorption capacity and rate of adsorption, respectively, and resolute from the linear plot of specific adsorption C_e/Q_e against the equilibrium concentration C_e . Figure-13 shows the Langmuir isotherm plots for the adsorption of MV6B onto the raw and acid activated clays. These values are listed in Table-1. There is a marked increase in the values of the adsorption capacity Q_m for the acid activated clays, which means that the activation improved the adsorption capacity for the raw clay. The ACS shows the optimal adsorption capacity Q_m , which is evidently higher than those of the ACH and RC samples. This confirms that the generation of more total binding sites leads to increase the porosity [24]. The significant feature of the Langmuir isotherm can be exhibited by R_s , a dimensionless equilibrium parameter or separation factor. R_s values are calculated from the equation $R_s = \frac{1}{1+K_L \cdot C_o}$. When the value of R_s is between 0 and 1, then the adsorption is favorable, while at $R_s > 1$ the adsorption is unfavorable, $R_s = 0$ reflects irreversible adsorption, and $R_s = 1$ indicates linear adsorption. Table-2 shows the values of $1 > R_s > 0$ for all samples, which indicates that the adsorption of MV6B dye onto clays is favorable [25].



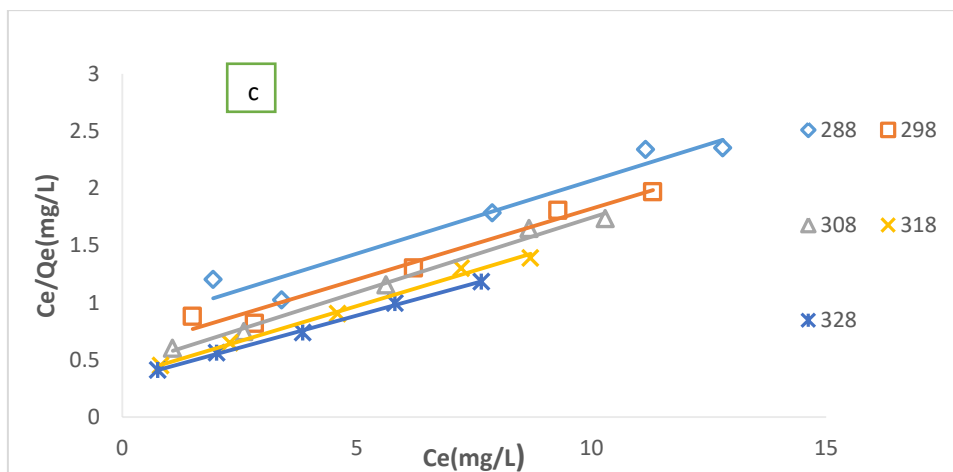


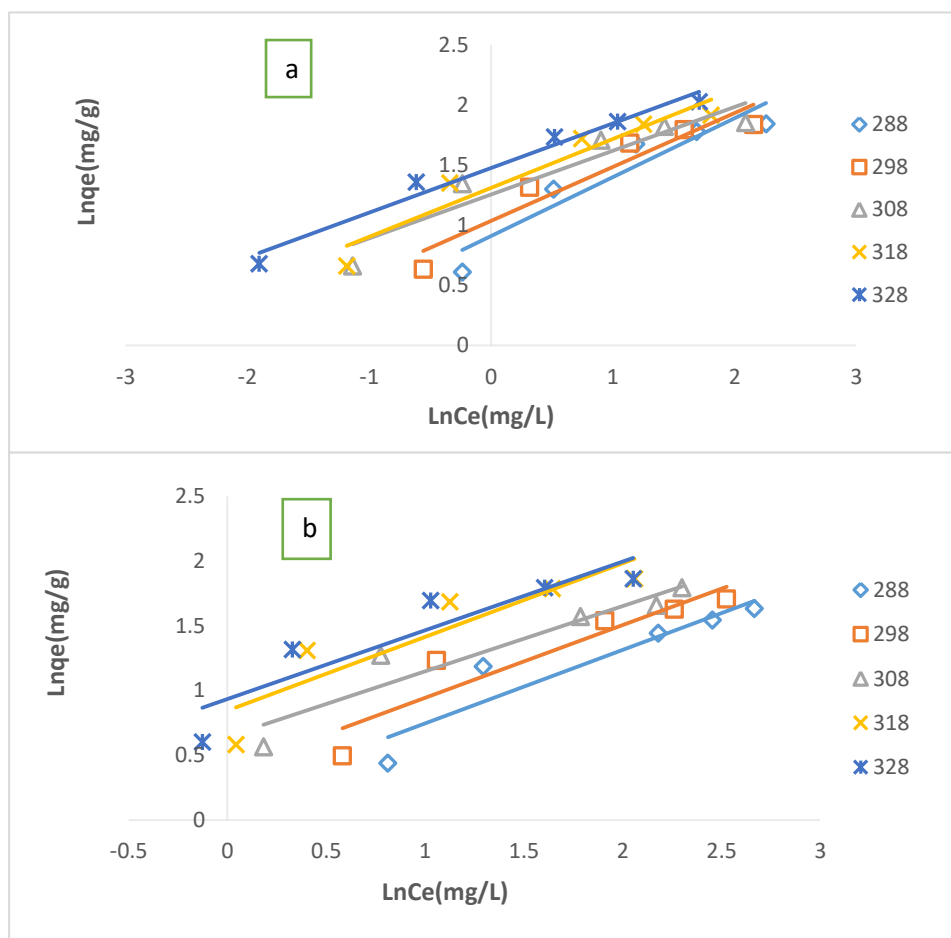
Figure 13- Langmuir isotherm plots for the adsorption of MV6B dye onto (a) RC, (b) ACH, and (c) ACS at different temperatures.

5-2- Freundlich isotherm

Freundlich model assumes that MV6B adsorption takes place on sites with various adsorption energies or at heterogeneous clay surfaces. It is usually written as [26]:

$$\ln q_e = \ln K_f + \frac{1}{n_f} \ln C_e \tag{4}$$

where K_f and n_f are Freundlich constants related to adsorption capacity and adsorption intensity, respectively. The values of these constants were estimated from the intercept and slope of the plot between $\ln q_e$ vs $\ln C_e$ (Figure-14), as illustrated in Table-1. The value of n_f identifies the favorability of the sorption process. If it is within the range of $1 < n_f < 10$, then the adsorption is favorable [18]. From the listed values of n_f , it is clear that it lies in the range of 1-10, verifying a favorable adsorption process.



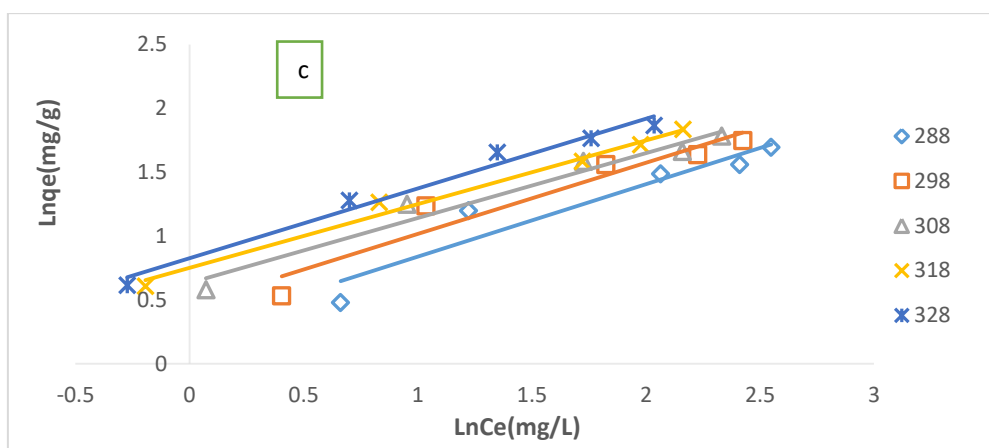


Figure 14- Freundlich isotherm plots for the adsorption of MV6B dye onto (a) RC, (b) ACH, and (c) ACS at different temperatures.

5-3- Temkin model

This model is based on the effects of the indirect dye- clay interactions on sorption. The heat of adsorption is decreasing linearly with the surface coverage [23]. The linear equation for Temkin isotherm is expressed as [18]:

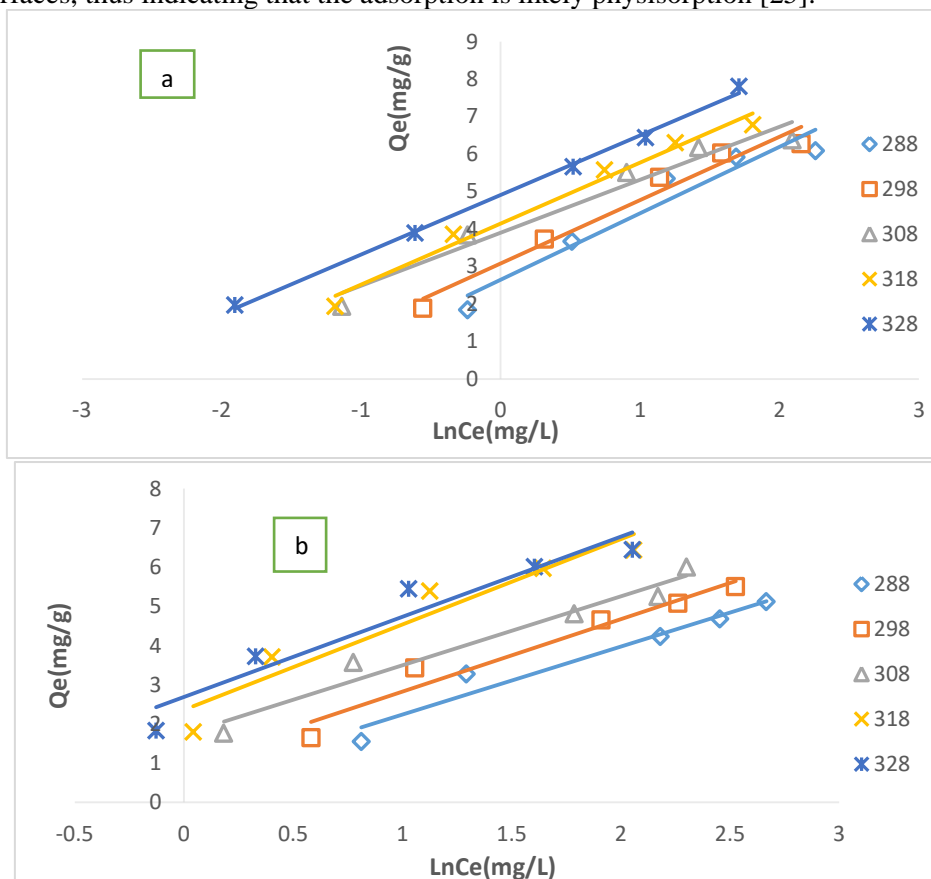
$$Q_e = B_T \ln A_T + B_T (\ln C_e) \quad \text{--- (5)}$$

where A_T = Equilibrium binding constant (L/g).

$B_T = \frac{RT}{b_T}$, (b_T in mol . K J⁻¹), is Temkin constant related to heat of adsorption.

R= universal gas constant (8.314 J.mol⁻¹.K⁻¹). T= absolute temperature (K).

The constants A_T and b_T are evaluated from the intercept and slope of the linear plot of Q_e vs. $\ln C_e$. The obtained values are listed in Table- 1. The positive values of b_T noted that the adsorption process is endothermic. The values of $B_T < 8$ KJ/mol indicate weak interaction between MV6B ions and clay sample surfaces, thus indicating that the adsorption is likely physisorption [25].



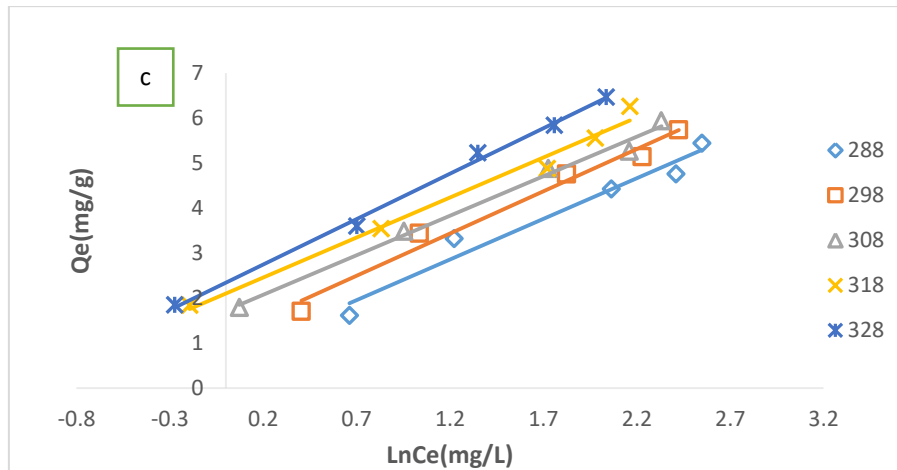


Figure15-Temkin isotherm plots for the adsorption of MV6B dye onto (a) RC, (b) ACH, and (c) ACS at different temperatures.

5-4- Dubinin-Radushkevich (D-R) isotherm

The Dubinin-Radushkevich isotherm was applied to study the adsorption on microporous materials based on the potential theory of adsorption. The linear form of D-R model is:

$$\ln Q_e = \ln K_{D-R} - B \epsilon^2 \tag{6}$$

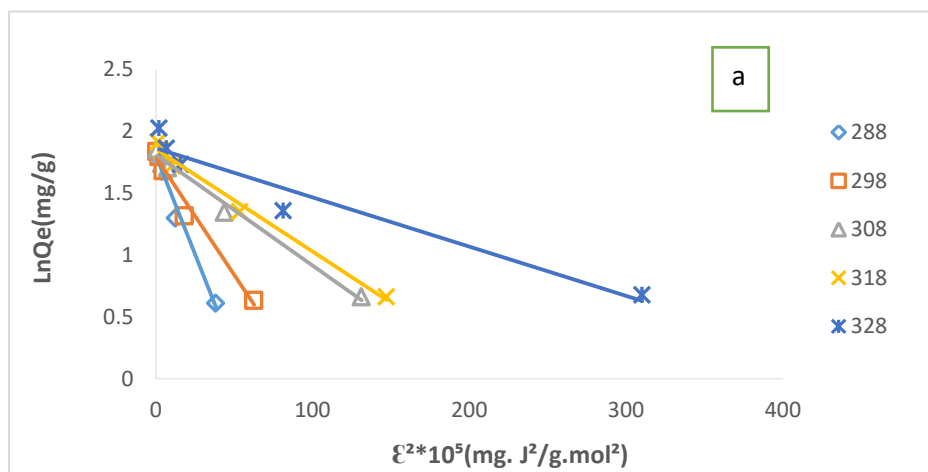
where B: activity coefficient related to the mean adsorption energy (mole²/KJ²).

K_{D-R} : maximum adsorption capacity (mg/g).

ϵ : polanyi potential calculated by using the equation $\epsilon = RT \ln [1 + 1/C_e]$.

The adsorption energy E (J/mole) is calculated by $E = - \frac{1}{(2B)^{0.5}}$.

When the value of E < 8 KJ/mole, the adsorption process is physical, whereas at E > 8 KJ/mole, the adsorption process is a chemisorption. The D-R parameters were calculated from the slope and intercept of $\ln Q_e$ vs. ϵ^2 and the values are given in Table-1. The value of E is almost lower than 8KJ/mol. It verifies that the MV6B adsorption on RC, ACH, and ACS is a physical one [25]. It is obvious that Langmuir isotherm described better the dye uptake, with the higher correlation coefficient R² values, for the RC, ACH, and ACS samples in comparison with that of the other adsorption isotherm models.



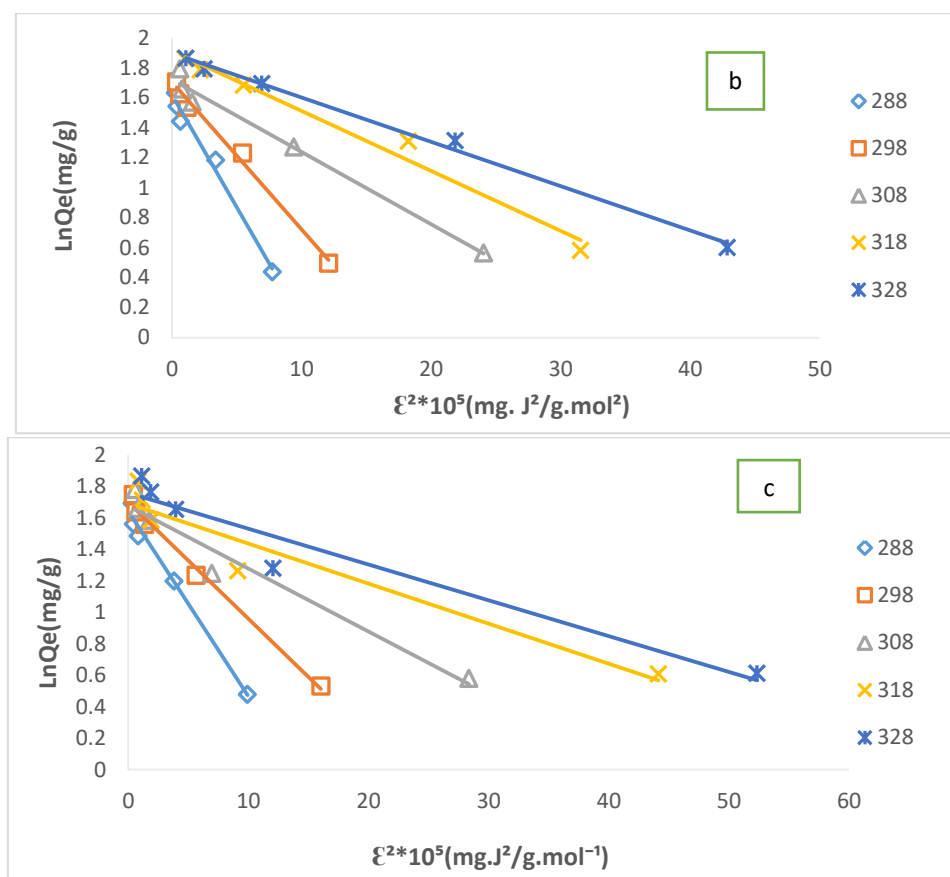


Figure16-D-R isotherm plots for the adsorption of MV6B dye onto (a) RC, (b) ACH, and (c) ACS at different temperatures.

Table 1- Equilibrium isotherm data for the adsorption of MV6B dye onto RC, ACH, and ACS at different temperatures.

Langmuir					Freundlich				
	Temperature (K)	Q_m (mg.g ⁻¹)	K_L (L/mg)	R^2	Slope (1/n _f)	n _f	Intercept LnK _{Fr}	K_{Fr} (mg/g)	R^2
RC	288	7.4570	0.5550	0.9819	0.4906	2.038	0.9086	2.4808	0.8882
	298	7.3909	0.7260	0.9942	0.4478	2.233	1.0357	2.8170	0.9099
	308	6.9930	1.4400	0.9988	0.3640	2.747	1.2545	3.5060	0.8925
	318	7.6982	1.2400	0.9991	0.4071	0.456	1.3098	3.7054	0.9172
	328	7.4738	2.1090	0.9995	0.3704	2.699	1.4748	4.3701	0.9725
ACH	288	7.5870	0.1430	0.9903	0.5675	1.762	0.1791	1.1961	0.8717
	298	7.7570	0.1940	0.9881	0.5608	1.783	0.3827	1.4662	0.8700
	308	7.1580	0.3350	0.9846	0.5037	1.985	0.6435	1.9031	0.9035
	318	7.9617	0.5670	0.9952	0.5681	1.760	0.8439	2.3254	0.8190
	328	8.5760	0.4390	0.9992	0.5309	1.883	0.9332	2.5426	0.8301
ACS	288	7.8490	0.1610	0.9824	0.5686	1.758	0.2698	1.3097	0.9021
	298	8.0710	0.2340	0.9896	0.5568	1.795	0.4598	1.5837	0.9193
	308	7.6680	0.2960	0.9904	0.5079	1.968	0.6344	1.8858	0.9611
	318	8.1230	0.3450	0.9925	0.4994	2.002	0.7513	2.1197	0.9865

	328	8.8880	0.3460	0.9979	0.5461	1.831	0.8265	2.2853	0.9779
Temkin									
RC	Temperature (K)	B_T (J. mol⁻¹)	b_T	Intercept	A_T (L/g)	R²			
	288	1.7760	1348.2	2.6453	4.4347	0.9306			
	298	1.6903	1465.7	3.0843	6.2009	0.9642			
	308	1.4130	1812.2	3.9048	15.8549	0.9569			
	318	1.6251	1626.8	4.1453	12.8173	0.9809			
	328	1.5874	1717.8	4.9105	22.0524	0.9970			
ACH	288	1.7366	1378.8	0.4999	1.3335	0.9482			
	298	1.8508	1338.6	0.9719	1.6906	0.9528			
	308	1.7600	1454.9	1.7344	2.6790	0.9589			
	318	2.1797	1212.9	2.3525	2.9425	0.9207			
	328	2.0466	1332.4	2.6845	3.7124	0.9230			
ACS	288	1.8080	1324.3	0.6890	1.4638	0.9604			
	298	1.8800	1317.8	1.1784	1.8716	0.9781			
	308	1.7593	1455.5	1.7197	2.6577	0.9906			
	318	1.7808	1484.6	2.0980	3.2482	0.9847			
	328	2.0198	1350.1	2.3439	3.1914	0.9957			
Dubinin- Radushkevich									
	Temperature (K)	B mol²/KJ²		E J/mol	K_{D-R} (mg/g)		R²		
RC	288	0.0321		3.9525	1.8071		0.9852		
	298	0.0190		5.1546	1.7887		0.9773		
	308	0.0090		7.4626	1.8109		0.9888		
	318	0.0083		7.7639	1.8567		0.9882		
	328	0.0040		8.2359	1.8621		0.9398		
ACH	288	0.1495		1.8315	1.6179		0.9842		
	298	0.0982		2.2573	1.7043		0.9911		
	308	0.0482		3.2258	1.7214		0.9828		
	318	0.0399		3.5460	1.9109		0.9798		
	328	0.0295		4.1186	1.8965		0.9947		
ACS	288	0.1178		2.0703	1.6432		0.9866		
	298	0.0740		2.6041	1.6989		0.9891		
	308	0.0400		3.5460	1.6778		0.9562		
	318	0.0254		4.4385	1.6916		0.9250		
	328	0.0228		4.6948	1.7599		0.9382		

Table 2- Dimensionless equilibrium parameters for the adsorption of MV6B dye onto RC, ACH, and ACS at different temperatures.

Temperature(K)	<u>RC</u>	<u>ACH</u>	<u>ACS</u>
	<u>Rs</u>		
288	0.1526	0.4115	0.6230
298	0.5793	0.5150	0.2994
308	0.0649	0.2290	0.2524
318	0.0746	0.1499	0.2240
328	0.0452	0.1855	0.2155

6- Adsorption thermodynamic

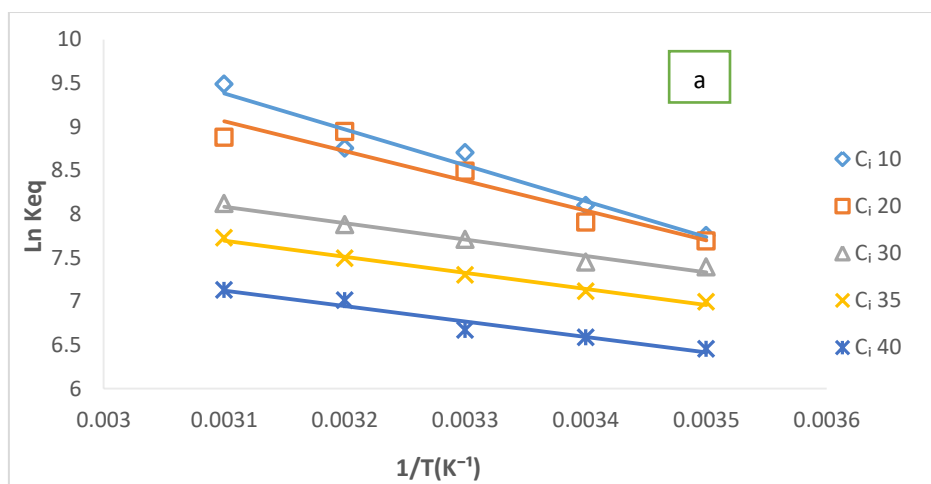
The thermodynamic parameters for the adsorption of MV6B were evaluated by using the following equations:

$$\Delta G = -RT \ln K_{eq} \text{----- (7)}$$

$$K_{eq} = \left[\frac{C_i - C_e}{C_e} \right] \left[\frac{V}{M} \right] \text{----- (8)}$$

$$\ln K_{eq} = \frac{\Delta S}{R} - \frac{\Delta H}{R} \cdot \frac{1}{T} \text{----- (9)}$$

where T is absolute temperature (K), K_{eq} is the ability of adsorbate to retain and a measure of its movement within solution, R is the perfect gas constant ($8.314 \text{ J.K}^{-1}\text{mol}^{-1}$), C_i and C_e are the initial and equilibrium concentrations, respectively, of MV6B dye solution (mg/L), M is the weight of the adsorbent (g), and V is the volume solution of adsorbate in (L) [27]. The values of ΔH°_a and ΔS°_a can be estimated from the slope and intercept of the linear Vant’s Hoff plot of $\ln K_{eq}$ vs. $1/T$, while the values of ΔG°_a can be estimated from equation 7 [28] (Figure-17 a, b, and c). Thermodynamic data for the adsorption of MV6B dye onto RC, ACH, and ACS are shown in Table- 3. The negative values of the Gibbes free energy ΔG°_a confirm that the adsorption of MV6B dye onto clays is spontaneous. The positive values of ΔH°_a confirm an endothermic nature for the sorption process, while the positive values of the entropy change ΔS°_a suggest an increase in randomness at the interface between solid/solution, which is related to the increase in the degrees of freedom of the dye species [18].



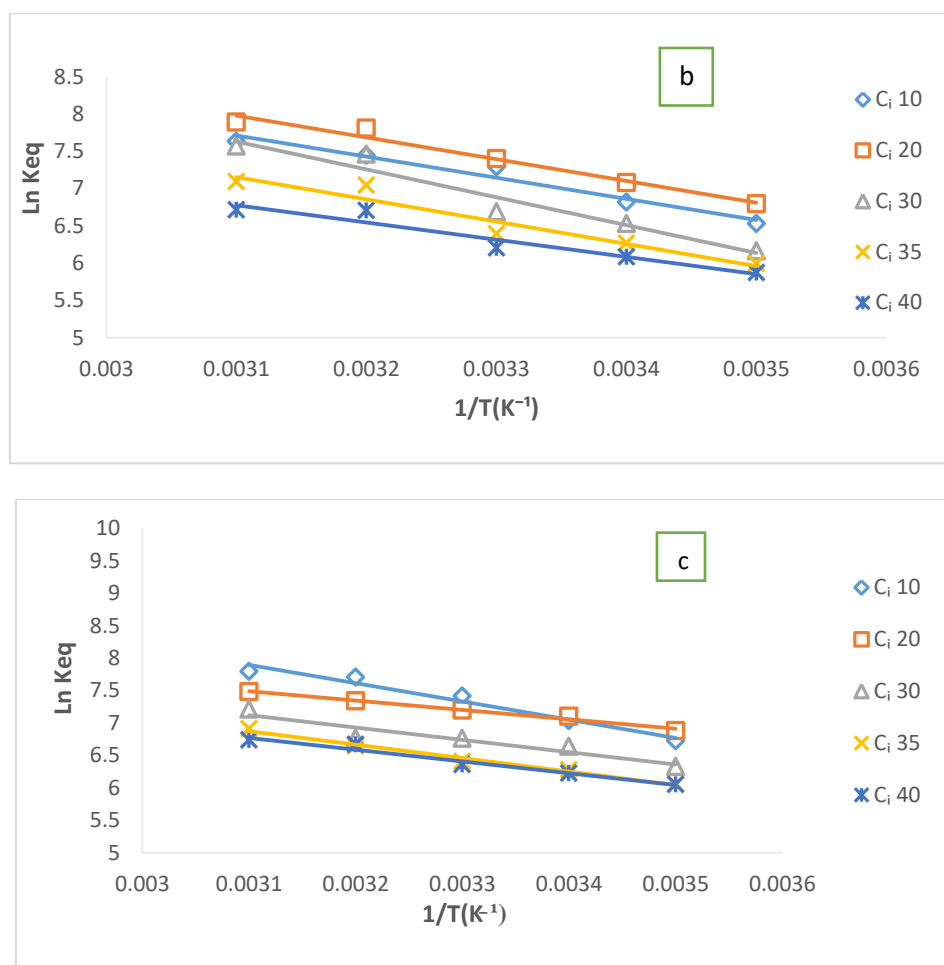


Figure17- Van't Hoff plots for the adsorption of MV6B dye onto (a) RC, (b) ACH, and (c) ACS at different temperatures.

Table 3- Thermodynamic parameters for the adsorption of MV6B dye onto raw clay and acid activated clays

	C _i (mg/L)	ΔH(kJ/mol)	ΔS(kJ/mol)	(-) ΔG(kJ/mol)				
				288K	298K	308K	318K	328K
RC	10.0	34.295	0.1843	18.56	20.06	22.28	23.14	25.87
	20.0	28.383	0.1633	18.41	19.58	21.73	23.64	24.21
	30.0	15.646	0.1157	17.70	18.45	19.73	20.83	22.13
	35.0	15.322	0.1114	16.74	17.62	18.70	19.81	21.07
	40.0	14.740	0.1049	15.45	16.31	17.07	18.53	19.43
ACH	10.0	23.545	0.1371	15.64	16.89	18.66	19.68	20.82
	20.0	24.268	0.1415	16.27	17.54	18.95	20.65	21.52
	30.0	31.086	0.1598	14.76	16.18	17.13	19.73	20.64
	35.0	24.759	0.1362	14.35	15.53	16.37	18.63	19.34
	40.0	19.197	0.1158	14.06	15.07	15.88	16.40	18.31
ACS	10.0	23.420	0.1382	16.09	17.42	18.98	20.37	21.25
	20.0	11.947	0.0993	16.48	17.60	18.43	19.40	20.41
	30.0	15.763	0.1080	15.15	16.45	17.32	17.90	19.66
	35.0	17.218	0.1105	14.50	15.55	16.40	17.56	18.84
	40.0	15.073	0.1030	14.49	15.43	16.27	17.63	18.37

7- Conclusions

Acid activation of clay mixture was successfully accomplished in the course of the investigation described. Both acid clays of ACH and ACS showed sufficient adsorption in respect to Methyl Violet 6B from aqueous solution, which may be related to the presence of different functional groups on their surfaces as well as their porous structure. These results lead to highest adsorption capacity obtained for the both types of acid-activated clays. The study of the impacts of the various variables revealed that the sorption process was dependent on clay dosage, agitation time, starting MV6B concentration, temperature, ionic strength, and pH values. Among the different adsorption isotherm models used, Langmuir model described better the uptake of MV6B dye by using ACH and ACS clays as adsorbents. Thermodynamic calculation indicated that the adsorption of MV6B on the clay samples was an endothermic and spontaneous process that occurs with the increase in the randomness.

References

1. Adeyemo, A.A., Adeoye, I.O. and Bello, O.S. **2015**. Adsorption of Dyes Using Different Types of Clay: A review, *Applied Water Science*, **20**(2): 453-568.
2. Ozcan, A.S., Erdem, B. and Ozcan, A. **2005**. Adsorption of Acid Blue193 from Aqueous Solutions onto BTMA-Bentonite, *Colloids and Surfaces A: Physicochemical and Engineering Aspects*, **266**(1-3): 73-81.
3. Bhatnagar, A. and Jain, A.K. **2005**. A comparative Adsorption Study with Different Industrial Wastes as Adsorbent for the Removal of Cationic Dyes from Water, *Journal of Colloid and Interface Science*, **281**(1): 49-55.
4. Adebowale, K.O., Owolabi, B.I. and Chigbundu, E.C. **2014**. Removal of Safranin-O from Aqueous Solution by Adsorption onto Kaolinite Clay, *Journal of Encapsulation and Adsorption Sciences*, **4**(3): 89-104.
5. Fungaro, D.A. and Magdalena, C.P. **2012**. Adsorption of Reactive Red 198 from Aqueous Solution by Organo Zeolite from Fly Ash: Kinetic and Equilibrium Studies, *International Journal of Chemical and Environmental Engineering Science*, **3**(3): 7-14.
6. Osman, A.I., Ahmed, A.T., Johnston, C.R. and Rooney, D.W. **2017**. Physicochemical Characterization of Miscanthus and its Application in Heavy Metals Removal from Wastewaters, *Environmental Progress and Sustainable Energy*, **37**(3): 1058-1067.
7. Zakaria R.M., Hassan, I., El-Abd, M.Z. and El-Towil, Y.A. **2009**. Lactic Acid Removal from Wastewater by Using Different Types of Activated Clay, *Thirteen International Water Technology Conference*, **13**: 403-416.
8. Rizk, S.E. and Hamed, M.M. **2015**. Batch Sorption of Iron Complex Dye, Naphthol Green B, from Wastewater on Charcoal, Kaolinite, and Tafla, *Desalination and Water Treatment*, **56**(6): 1-11.
9. Mohamed, S.S. and Al-Heetimi, D.T.A. **2019**. Adsorption of Methyl Violet Dye from Aqueous Solution by Iraqi Bentonite and Surfactant – Modified Iraqi Bentonite, *Ibn Al Haitham Journal for Pure and Applied Sciences*, **23**(3): 28-42.
10. Sejie, F.P. and Tabbiruka, M.S. **2016**. Removal of Methyl Orange (MO) from Water by Adsorption onto Modified Local Clay (Kaolinite), *physical chemistry*, **6**(2): 39-48.
11. Lu, P., Chen, T., Liu, H., Li, P., Peng, S., Yang, Y. and Green, **2019**. Preparation of Nanoporous Pyrrhotite by Thermal Treatment of Pyrite as an Effective Hg (II) Adsorbent: Performance and mechanism, *Minerals*, **9**(2): 1-17.
12. Vollprecht, D., Fruhauf, S., Stocker, K. and Ellersdorfer, M. **2019**. Ammonium Sorption from Landfill Leachates Using Natural and modified Zeolites: Pre-Testes for a Novel Application of the Ion Exchanger Loop stripping process, *Minerals*, **9**(8):1-10
13. Eskhan, A., Banat, F., Selvaraj, M. and Abu Haija, M. **2019**. Enhanced Removal of Methyl Violet 6B Cationic Dye from Aqueous Solutions Using Calcium Alginate Hydrogel Grafted with Poly (Styrene-co-Maleic Anhydride), *Polymer Bulletin*, **76**(1): 175-203.
14. AL-Dabbagh, N.O.F. **2018**. Minerology and Geochemistry of Injana and Mukdadiya Formations (Upper Miocene-Pliocene) in Zorbatiya area, east Iraq. M.Sc. Thesis, University of Baghdad, Baghdad, Iraq.

15. Obiageli, A.R. **2017**. Adsorption of Cationic Dye onto Low-Cost Adsorbent Synthesized from Bentonite Clay Part 1. Kinetic and Thermodynamic Studies, *Journal of Chemical Technology and Metallurgy*, **52**(3): 491-504.
16. Allam, K., Gourai, K., EL Bouari, A., Belhorma, B. and Bih, L. **2018**. Adsorption of Methylene Blue on Raw and Activated Clay: Case Study of Bengurir Clay, *Journal of Materials and Environmental Sciences*, **9**(6): 1750-1761.
17. Miyah, Y., Lahrichi, A., Idrissi, M., Anis, K. and Kachkoul, R. **2017**. Removal of Cationic Dye “ Crystal Violet ” in Aqueous Solution by the Local Clay, *Journal of Materials and Environmental Sciences*, **8**(10): 3570-3582.
18. Collins, O.N., Elijah, O.C. and Okechhukwu, O. **2019**. Adsorption of a Dye (Crystal Violet) on an Acid Modified on- Conventional Adsorbent, *Journal of Chemical Technology and Metallurgy*, **54**(1): 95-110.
19. Lamayi, D.W., Shehu, Z. and Kwarson, P.S. **2018**. Aqueous Phase Removal of Fluoride as Fluorosis Agent Using Montmorillonite Clay as Natural Nano Adsorbent, *Nano chemistry Research*, **3**(2): 219-226.
20. Zhang, Y., Wang, D., Liu, B., Cao, X., Xu, W. and Liang, P. **2013**. Adsorption of Fluoride from Aqueous Solution Using Low-Cost Bentonite/ Chitsan Beads, *American Journal of Analytical Chemistry*, **4**(7): 48-53.
21. Al-Rudaini, K.A. **2017**. Adsorption Removal of Rhodamine-B Dye from Aqueous Solution Using Rhamnus Stone as Low Cost Adsorbent, *Journal of Al-Nahrain University*, **20**(1): 32-41.
22. Khalid, E., Laachach, A., Alaoui, A. and Azzi, M. **2011**. Removal of Methyl Violet From Aqueous Solution Using a Stevensite-Rich Clay from Morocco, *Applied Clay Science*, **54**(1): 90-96.
23. Bouatay, F., Dridi, S. and Mhenni, M.F. **2014**. Valorization of Tunisian Pottery Clay onto Basic Dyes Adsorption, *International Journal of Environmental Researches*, **8**(4): 1053-1066.
24. Ogbaji, E.G., Hikon, B.N., Sheckhar, N.G., Yerima, E.A., Mavis, O., Ekirigwe, O. and Ayodeji, A.F. **2019**. Synergistic Study of Hydroxyiron (III) and Kaolinite Composite for the Adsorptive Removal of Phenol and Cadmium, *International journal of Environmental Chemistry*, **3**(1): 30-42.
25. Emeniru, D.C., Onukwuli, O.D., Wodu, P.D. and Okoro, b.I. **2015**. The Equilibrium and Thermodynamics of Methylene Blue Uptake onto Ekowe Clay; Influence of Acid Activation and Calcination, *International Journal of Engineering and Applied Sciences*, **2**(5): 17-25.
26. Atiya, M.A., M-Ridha, M.J. and Saheb, M.A. **2020**. Removal of Aniline Blue from Textile Wastewater Using Electrocoagulation with the Application of the Response Surface Approach, *Iraqi Journal of Science*, **61**(11): 2797-2811.
27. Bendaho, D., Driss, T.A. and Bassou, D. **2017**. Adsorption of Acid Dye onto Activated Algerian Clay, *Bulletin of the Chemical Society of Ethiopia*, **31**(1): 51-62.
28. Sumaila A., Ndamitso M.M., Iyaka Y.A., Abdulkareem A.S., Tijani J.O. and Idris M.O. **2020**. Extraction and Characterization of Chitosan from Crab Shells: Kinetic and Thermodynamic Studies of Arsenic and Copper Adsorption from Electroplating Wastewater, *Iraqi Journal of Science*, **61**(9): 2156-2171.